Original Article

Investigating the effect of the nitric oxide donor L-arginine on albendazole efficacy in *Trichinella spiralis*-induced myositis and myocarditis in mice

Magda S Abdeltawab[1], Iman R Abdel-Shafi[1], Basma E Aboulhoda[2], Hanaa Wanas[3], Shimaa Saad El-Din[4], Samar I Amer[5], Alshaimaa M Hamed[1]

Departments of Medical Parasitology[1], Anatomy and Embryology[2], Pharmacology[3], Biochemistry[4], Pathology[5], Faculty of Medicine, Cairo University, Cairo 11956, Egypt

ABSTRACT

Background: The immune response against *Trichinella spiralis* results in a mixed cytokine state and nitric oxide (NO) production. Albendazole (ALB) influences the oxidative status and cytokine profile of the host, in addition to its direct action on the parasite β-tubulin.
Objective: The current study was designed to assess the effect of the NO donor, L-arginine, on the muscular phase of experimental trichinosis in mice with and without ALB administration.
Material and Methods: The study included five groups (G); negative non-infected control group (G1); positive infected non-treated control group (G2); ALB-treated group (G3); L-arginine-treated group (G4); and combined ALB and L-arginine regimen group (G5). Study parameters included larval count, histopathological changes, and NO synthase (iNOS) immunohistochemical expression in skeletal muscle and heart during the muscular phase. Gene expression levels of tumor necrosis factor-α (TNF-α), interferon-γ (IFN-γ), and β-tubulin, as well as NO production were evaluated by quantitative real time PCR (RT-qPCR).
Results: L-arginine resulted in a significant increase in tissue iNOS expression and serum NO levels, in addition to the increase in TNF and INF gene expression. Albendazole, on the other hand, was found to decrease local tissue expression of iNOS and serum NO in infected mice, whereas gene expression levels of TNF and IFN were elevated.
Conclusion: Nitric oxide homeostasis is vital to the infection outcome and regeneration during muscular trichinosis. Albendazole exerts immunomodulatory effects in addition to its direct anti-parasitic action on *T. spiralis*.

Keywords: Albendazole; immunohistochemistry; inflammation; L-arginine; muscular phase; nitric oxide; RT-qPCR; trichinosis.

Received: 2 February, 2022; **Accepted:** 28 March, 2022.

Corresponding Author: Alshaimaa M. Hamed, **Tel.:** +20 1026893667, **E-mail:** amsolaiman@kasralainy.edu.eg

Print ISSN: 1687-7942, **Online ISSN:** 2090-2646, **Vol. 15, No. 1, April, 2022.**

INTRODUCTION

Trichinella spp. are unique helminths that parasitize the same definitive and intermediate animal and human hosts establishing themselves in protected intracellular niches in their hosts' muscles. The adult worm lodges in a peculiar multi-intracellular fashion in the small intestinal enterocytes[1]. They release newborn larvae that enter the blood stream and settle in skeletal muscles where they become infective larvae (L1), transforming the hosting muscle fibers into a permanent residence[2]. The parasitized muscle cell becomes enslaved by its new occupier, where its genetic and metabolic machinery becomes devoted to the foundation and maintenance of a nourishing and protective environment for the larvae. The muscle fibers transform into complex apparatuses called nurse cells or nests. These are formed of a host-derived collagen capsule, which ensures protection, and a host-derived cellular component that provides the metabolic requirements for the nesting larvae[3]. The formation of nurse cells is a unique process for skeletal muscles. Larvae of *T. spiralis* are unable to encyst in other types of cells including myocardial muscle cells. The cardiac pathology during trichinosis is due to the anti-*Trichinella* immune response that results in eosinophilic myocarditis[4].

This parasitic occupation does not remain without counter-resistance by the host. A humoral immune reaction occurs in response to various parasite antigens, the most famous of which is the sugar-antigen tyvelose. A predominantly IgG1, IgG2 and IgE response prevails during the chronic phase of trichinosis[5]. The cell-mediated immune response results in a mixed cytokine state, where IL-10, IL-5 and IFN-ɣ were found to persist for up to 3 years post-infection[6].

In addition to the production of cytokines, the immune response to trichinosis also includes NO production which when combined with oxygen free

 DOI: 10.21608/puj.2022.119638.1153

radicles forms peroxy-nitrite, a substance injurious to muscle cells[7]. Notably, NO is produced by nitric oxide synthase (NOS) from the semi-essential amino acid arginine, which is involved in various biological functions involving immunity, inflammation and wound repair[8]. Exogenous supplementation with dietary arginine was found to increase the activity of inducible NOS (iNOS) and thus elevate serum NO levels[9]. Regulation of NO synthesis is achieved by lipopolysaccharide and various cytokines such as IFN-γ and TNF-α, which are important activators for macrophages to produce NO[10].

Arginine is also metabolized by parasites as reported by Das *et al*.[11] in their interesting review on the modulation of arginase pathway by pathogenic organisms. They stated that parasites can choose to divert the host arginine pool as a survival strategy and that the competition between iNOS and arginase for arginine can contribute to the outcome of several parasitic and bacterial infections. For instance, *G. lamblia* can utilize arginine by its own enzymes, thus interfering with the production of the lethal NO molecule. Supplementation with exogenous arginine was found to partially restore NO levels *in vitro*[12].

Benzimidazoles are a group of antiparasitic agents that form the cornerstone of trichinosis management. This group includes agents such as albendazole, mebendazole and thiabendazole and acts by binding to parasite β-tubulin thus inhibiting microtubule polymerization[13]. These drugs do not only affect the parasite, but also influence various biological processes in the infected host. Of particular importance is the effect of benzimidazoles on the immune response. Albendazole has been reported to influence the oxidative status and cytokine profile of the host[7,14]. In the current study, we investigated the effect of the NO precursor L-arginine on infection outcome and treatment efficacy, in addition to the impact of ALB-induced immunomodulation during the muscular phase of trichinosis in mice on both skeletal and cardiac muscle.

MATERIAL AND METHODS

The current work is an experimental case-control study conducted in Medical Parasitology and Pharmacology Departments, and animal house of the Faculty of Medicine, Cairo University during the period between November 2017 and June 2018.

Study design: Mice were infected with *T. spiralis* larvae and according to mice grouping, they were treated either with L-arginine, or ALB, or a combined regimen. Mice were sacrificed 30 days post-infection (PI) by cervical dislocation under anesthesia to study changes during the muscular phase of infection. Results were compared with non-infected and infected non-treated mice. Evaluated parameters included larval parasite load, histopathological examination of skeletal and cardiac muscles, local iNOS tissue expression and serum NO levels.

Strain: *T. spiralis* larvae were generously provided by Medical Parasitology Department, Faculty of Medicine, Tanta University, and were obtained originally from the Cairo abattoir from infected pig muscles. The life cycle was initiated and maintained by successive passages in parasite-free BALB/C mice.

Experimental animals: The study included forty parasite-free male BALB/C mice, 6-8 w old and 20-25 g body weight (BW). Mice were bred under standard conditions; 25±2°C room temperature, 12-hour light/dark cycle, and free access to standard pellet diet and water ad libitum.

Drugs preparation, and dosage: Both drugs; ALB (20 mg/ml suspension), and L-arginine were purchased from Bendax, Sigma Pharmaceutical Industries, Egypt, and A8094 Sigma-Aldrich, Germany, respectively. To prepare ALB, every 10 ml were added to 30 ml of saline to reach the concentration of 5 mg/ml and each mouse in the ALB subgroup received 0.1 ml/10 g BW/day orally to reach the dose of 50 mg/kg/d[15]. L-arginine stock solution was supplied in powder form and dissolved in saline to prepare a concentration of 20 mg/ml, then each mouse in the L-arginine subgroup received 0.1 ml/10 g BW/d orally to reach the dose of 200 mg/kg/d. The control subgroups were given 0.1 ml/10 g BW normal saline orally by modified stomach tube and sacrificed at the end of the dosed treatment period.

Mice infection: Animals were exposed to an infective dose of 250±10 *T. spiralis* larvae per mouse by gastric feeding after a 12 h period of starvation[16].

Study animal groups: Mice were divided into five groups (8 mice each), that included two control groups: negative non-infected (G1), and positive infected non-treated mice that received oral saline from day 16 PI for 10 d (G2). Groups (G3 and G4) included ALB-treated mice that received an oral dose of 50 mg/kg/d ALB from day 21 PI for 5 d[15], and L-arginine-treated mice that received an oral dose of 200 mg/kg/d L-arginine from day 16 PI for 10 d[17], respectively. The last group (G5) received a combined ALB and L-arginine regimen composed of an oral dose of 200 mg/kg/d L-arginine from day 16 PI for 10 d combined with an oral dose of 50 mg/kg/d ALB from day 21 PI for 5 d[18].

Parameter assessment: Blood samples were collected for measuring serum NO level. Muscle tissue samples were snipped from *Rectus abdominus* for larval count, the gastrocnemius muscle, diaphragm, and heart for histopathological and immunohistochemical examination, and from the gastrocnemius muscle for

molecular analysis. The effect of ALB and L-arginine on the larvae, inflammation, and muscle degeneration in *T. spiralis* infected mice was analyzed according to the work plan in figure (1).

Parasitological examination for larval count[7]: Muscle parts from each mouse were dissected and individually incubated in equal volumes of 1% pepsin and 1% HCl in distilled water, at 37°C for 2 hours with intermittent agitation using an electric stirrer. Coarse particles were first removed from the digested product on a 50 mesh/inch sieve, then larvae were collected on a 200 mesh/inch sieve, washed twice, and suspended in 150 ml tap water in a conical flask. After allowing the larvae to sediment, the supernatant fluid was discarded, and the larvae were recovered and counted per ml under the microscope.

Histopathological examination of infected muscle tissue: The gastrocnemius muscle, diaphragm and heart samples were fixed in 10% formalin and embedded in paraffin blocks. Sections of 5 mm thickness were deparaffinized, rehydrated, stained with haematoxylin and eosin (H&E), and examined for interstitial infiltration and muscle degeneration[19]. The histopathological findings were graded as follows: no changes (–), mild changes with less than 10% of tissue section affected (+), moderate changes with 10–50% of tissue affected (++), and severe changes affecting more than 50% of the tissue section (+++)[20,21].

Immunohistochemical assessment of iNOS expression in muscle tissue: Following routine paraffin preparation and microwave antigen retrieval, sections from skeletal and myocardial muscle tissue were incubated in bovine serum albumin (BSA) and dissolved in PBS to prevent nonspecific background staining. The primary antibody used was rabbit polyclonal anti-iNOS antibody (1:100, ab15323-Abcam, USA), the secondary antibody was goat anti-rabbit IgG H&L (HRP) (ab205718). Mouse spleen tissue of positive control (G2) was similarly processed[22,23]. Photographs were obtained by an Olympus IX51 light microscope equipped with a DP72 device camera. The area percent of immunohistochemical staining was quantitatively studied in 6 fields/slide for each group using Leica Qwin 500 image analyser computer system (Cambridge, UK)

Assessment of serum NO levels[24]: Measurement of serum NO levels was performed using a colorimetric assay kit (BioVision Incorporated, CA, USA) according to the manufacturer`s recommendations. Briefly, in a microtiter plate, a series of prepared standards, sample blank, and 85 µL of each serum sample were dispensed. The test was performed in two steps. In the first step, 5 µL of each nitrate reductase mixture and enzyme co-factor were added to the sample and standard wells. The plate was incubated for 60 min to convert nitrate to nitrite, followed by another incubation for 10 min after adding 5 µL of the enhancer. In the second step, 50 µL of each Griess reagent R1 and R2 were added to convert nitrite into a deep purple compound. The absorbance was measured at 450 nm, plotted, and calculated from the standard curve.

Quantitative real time PCR (qRT-PCR) for TNF-α and IFN-γ gene expression in infected muscle tissue[25,26]: The gastrocnemius muscle tissue was minced and homogenized in a lysis buffer then transferred to a binding column to proceed to RNA isolation using GF-1 Nucleic Acid Extraction Kit (Vivantis Technologies, Malaysia), according to the manufacturer's protocol. The eluted total RNA was quantified by spectrophotometry. Reverse transcription was then performed by QuantiTect Reverse Transcription Kit (Qiagen, Germany), generating complementary DNA (cDNA) from 14 µl of the measured RNA. The relative abundance of the mRNA species was assessed by the SYBR Green method and an ABI Prism7500 Sequence Detector System (Applied Biosystems, USA). All cDNA, including the prepared samples for TNF-α and IFN-γ gene expression, β-actin gene expression serving as internal control, and non-template control, were run in duplicate. The primers used were designed with gene runner software from RNA sequences in GenBank

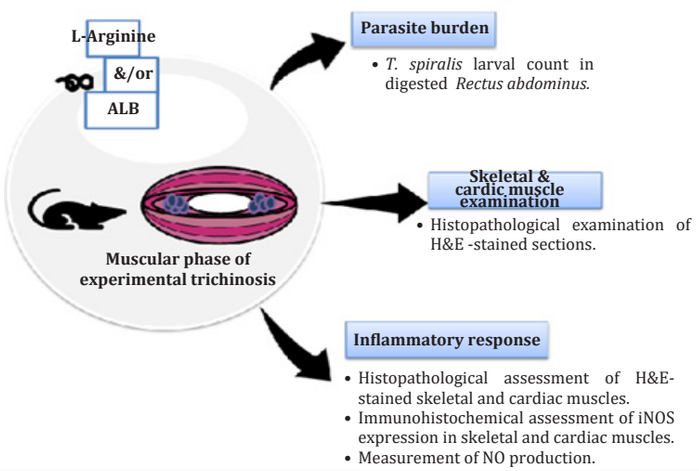

Fig. 1. Schematic presentation of study plan.

(Table 1). Quantitative RT-PCR analysis was performed in a 25 µl reaction volume consisting of 2× SYBR Green PCR Master Mix (Applied Biosystems, USA), 900 nM of each primer, and 2–3 µl of cDNA. The amplification conditions were 2 min at 50°C, 10 min at 95°C, and 40 cycles of denaturation at 95°C for 15 sec and annealing/extension at 60°C for one min. Data from the real-time assays were analyzed by Sequence Detection Software version 1.7 (PE Biosystems, USA). The relative expression levels of TNF-α and IFN-γ were calculated by the comparative threshold cycle (Ct) method according to the manufacturer recommendations (Applied Biosystems, USA).

Table 1. Primer sequences of the studied genes.

Parameter	Primers
TNF-α	**Forward:** 5′ GACGTGGAAGTGGCAGAAGAG 3′ **Reverse:** 5′ TGCCACAAGCAGGAATGAGA
IFN-γ	**Forward:** 5′ CGGCACAGTCATTGAAAGCCTA 3’ **Reverse:** 5′ GTTGCTGATGGCCTGATTGTC 3′
β-tubulin	**Forward:** 5’ GGCTGTATTCCCCTCCATCG 3' **Reverse:** 5′ CCAGTTGGTAACAATGCCATGT 3'

Statistical analysis: Data was presented as mean and standard deviation (SD). They were analyzed by the SPSS 25 software version. Comparison between groups was done using analysis of variance (ANOVA), in addition to Bonferroni post-hoc test for multiple comparisons. *P* values <0.05 were considered statistically significant.

Ethical consideration: All the animal housing, rearing and experiments were performed in the animal house of the Faculty of Medicine, Cairo University (Egypt), and were implemented in strict accordance with approved national and institutional guidelines.

RESULTS

Effect of ALB, L-arginine, and the combined regimen on larval count: When compared with the control infected non-treated G2, ALB effectively decreased the number of larvae in digested *Rectus abdominus* muscles in the ALB-treated G3 by 95.5%, while L-arginine induced an opposite effect with a significantly higher number of larvae in the L-arginine-treated G4 (51.8% increase). Mice receiving both ALB and L-arginine (G5) showed a significant decline in parasitic burden (by 69.6%). Pairwise comparisons between the groups showed statistical significance at *P*<0.05 (Table 2).

Histopathological changes during the muscular phase of experimental trichinosis treated with ALB (G3) and /or L-arginine (G4, G5)

Diaphragm: H&E-stained sections of the control G1 showed transversely sectioned polygonal muscle fibres with peripheral nuclei, acidophilic sarcoplasm surrounded by perimysium. The infected non-treated G2, showed numerous of *T. spiralis* larval cysts with granuloma formation, fibrous tissue deposition in the epimysium and thickened capsule of the encysted larvae. The ALB-treated G3 showed multiple completely degenerated larvae and very few viable ones. Degenerated encysted larvae appeared as a homogenous acidophilic substance replacing the larval structure. The arginine treated G4 demonstrated invasion of the larval cysts with dense mononuclear inflammatory cells. The combined ALB/L-arginine-treated G5 showed structural improvement in the diaphragm architecture with mild inflammation (Fig. 2; Table 3).

Gastrocnemius muscle: H&E-stained sections of the control group showed the classical architecture of the gastrocnemius muscle with longitudinally arranged parallel muscle fibres containing elongated vesicular nuclei, acidophilic sarcoplasm with flattened nuclei of fibroblasts in the endomysium and the overlying perimysium. The infected non-treated G2 showed *T. spiralis* larvae embedded in the muscle fibres with multiple foci of inflammatory infiltration and areas of fragmented degenerated muscle fibers. The larvae appeared encapsulated and surrounded by mononuclear cells. The ALB-treated G3 showed marked larval degeneration. The L- arginine-treated G4 showed mature *T. spiralis* larvae surrounded by thickened intact capsule and intense inflammatory infiltration. The combined ALB/L-arginine-treated G5 demonstrated

Table 2. Number of *T. spiralis* larvae in *Rectus abdominus* muscles of mice per ml of digested tissue.

	Larval count in digested *Rectus abdominus* muscles			Statistical analysis
	Mean ± SD	**Range**	**Change %**	***P* value**
Infected non-treated (G2)	56.0 ± 5.8	50-60	100%	**<0.001***
ALB-treated (G3)	2.5 ± 5.0	0-10	95.5% reduction	
L-Arginine-treated (G4)	85.0 ± 5.8	80-90	51.8% increase	
ALB/L-Arginine-treated (G5)	17.0 ± 5.0	10-20	69.6% reduction	

***:** Statistical significance (*P*<0.05).

Table 3. The severity of histopathological changes in diaphragm muscle tissue.

	Non-infected control (G1)	Infected non-treated (G2)	ALB-treated (G3)	L-Arginine-treated (G4)	Combined treatment (G5)
Larval degeneration	-	-	+++	+	++
Interstitial infiltration	-	++	+	+++	++
Capsular inflammation	-	++	-	+++	+
Muscle degeneration	-	++	+	+	+

partial larval degeneration, where the larvae appeared vacuolated with invasion of the larval substance and capsule with mononuclear inflammatory cells (Fig. 3).

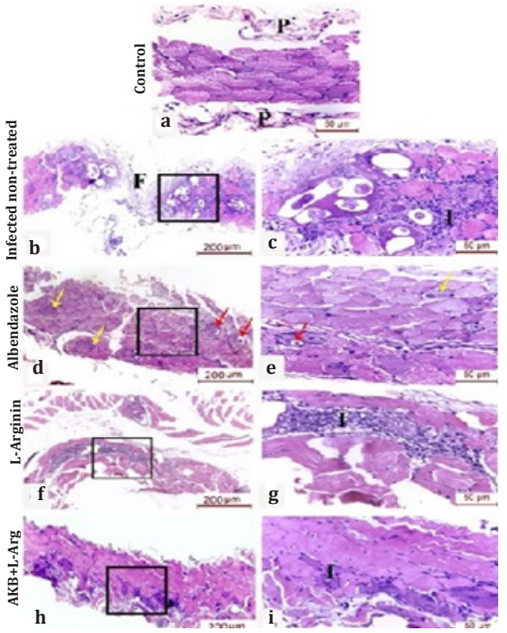

Fig. 2. H&E-stained sections of the diaphragm. **(a)** Control non-infected non-treated G1 showing normal architecture of the diaphragm's transversely sectioned polygonal muscle fibers with peripheral nuclei, acidophilic sarcoplasm, and surrounding perimysium. **(b)** Infected non-treated G2 showing multiple depositions of *T. spiralis* larval cysts (arrows) with granuloma formation and increased fibrous tissue deposition in the epimysium. **(c)** Higher magnification demonstrating mononuclear cell infiltrates surrounding the thickened capsule of the encysted larvae embedded in the diaphragm musculature. **(d)** ALB-treated (G3) and **(e)** higher magnification showing multiple completely degenerated larvae (yellow arrows) and very few viable ones (red arrows). **(f)** L-arginine-treated (G4) and **(g)** higher magnification, showing invasion of the larval cysts with dense mononuclear inflammatory cells. **(h)** Combined ALB/L-arginine-treated (G5) and **(i)** higher magnification, showing structural improvement in the architecture of the diaphragm musculature with mild inflammation. **F:** fibrous tissue, **I:** inflammatory infiltration, **P:** perimysium. [**a, c, e, g, i:** magnification x400, scale bar 50 µm, and **b, d, f, h:** magnification x100, scale bar 200 µm].

Myocardium: H&E-stained sections of the myocardium of the control (G1) showed branching and anastomosing cardiac muscle fibres with faint striations and abundant eosinophilic cytoplasm. The infected non-treated (G2) showed areas of cardiomyocyte degeneration replaced by dense inflammatory cellular infiltration. The ALB-treated (G3) showed wavy myocardial fibres arranged as branched interlacing bundles with dark apoptotic nuclei and focal areas of myocardial fibre separation. The L-arginine-treated (G4) displayed intact myocardial fibres with limited inflammatory infiltration. The nuclei appeared vesicular with

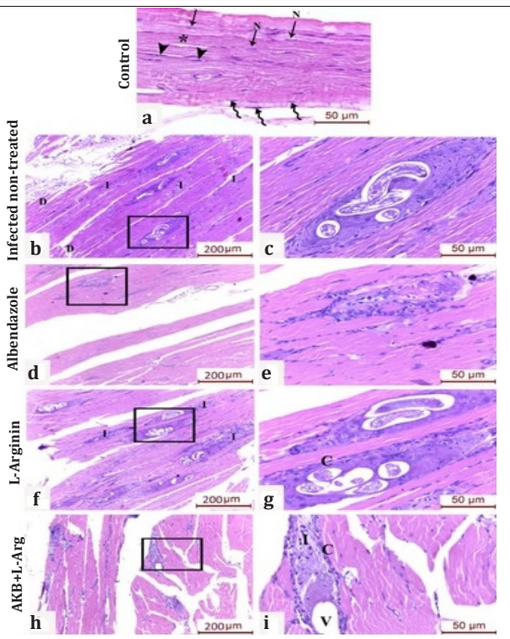

Fig. 3. H&E-stained sections of gastrocnemius muscle. **(a)** Control non-infected non-treated (G1) showing normal architecture of the gastrocnemius muscle with longitudinally arranged parallel muscle fibers containing elongated vesicular nuclei and acidophilic sarcoplasm (asterisk). Note flattened nuclei of fibroblasts in the endomysium (arrowhead) and the overlying perimysium (spiral arrow). **(b)** Infected non-treated (G2) demonstrating *T. spiralis* larvae embedded in the muscle fibers with multiple foci of inflammatory infiltration and areas of fragmented degenerated muscle fibers. **(c)** Higher magnification showing encysted encapsulated larvae surrounded by mononuclear cells. **(d)** ALB-treated (G3) revealing obvious decrease in the larval count with marked larval degeneration. **(e)** Higher magnification showing dead homogenized larva with capsular degeneration. **(f)** L-arginine-treated (G4) revealing marked increase in the count of larval infection with intense inflammatory infiltration. **(g)** Higher magnification depicts mature *T. spiralis* larvae surrounded by thickened intact capsule. **(h)** Combined ALB/L-arginine-treated (G5) showing partial larval degeneration. **(i)** Higher magnification demonstrating vacuolated larva with invasion of the larval substance and capsule with mononuclear inflammatory cells. **C:** capsule, **D:** degenerated muscle fibers, **F:** fibrous tissue, **I:** inflammatory infiltration, **L:** larvae, **P:** perimysium, **N:** nuclei, **V:** vacuolated larva, V. [**a, c, e, g, i:** magnification x400, scale bar 50 µm, and **b, d, f, h:** magnification x100, scale bar 200 µm].

irregular outline. The combined ALB/L-arginine-treated (G5) showed regular architecture of cardiomyocytes with very minimal inflammation (Fig. 4).

Immunohistochemical expression of iNOS in the gastrocnemius muscle, myocardium, and diaphragm: ALB therapy alone (G3) resulted in reduction in iNOS expression in the gastrocnemius muscle, myocardium and diaphragm as compared to the infected non-treated group (G2). Expression of iNOS in infected muscle tissue was found to be highest in L-arginine-treated mice (G4), followed by muscles from mice receiving both ALB and L-arginine (G5) (Fig. 5-10).

Effect of ALB, L-arginine and the combined regimen on the level of nitric oxide (NO) in the serum: Serum

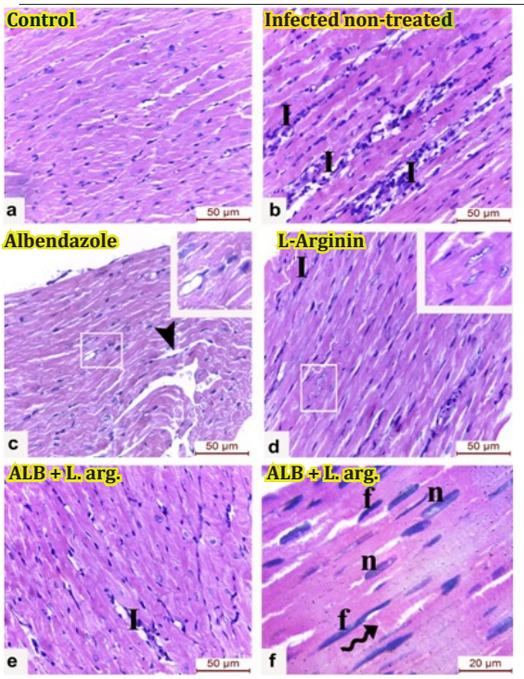

Fig. 4. H&E-stained sections of the myocardium. **(a)** Control (G1) showing normal histoarchitecture of the heart with branching and anastomosing cardiac muscle fibres with faint striations and abundant eosinophilic cytoplasm. **(b)** Infected non-treated (G2) shows areas of cardiomyocyte degeneration replaced by dense inflammatory cellular infiltration. **(c)** ALB-treated (G3) showing wavy myocardial fibres arranged as branched interlacing bundles with focal areas of myocardial fibre separation (arrowhead). The inset shows dark apoptotic nuclei. **(d)** L-arginine-treated (G4) showing intact myocardial fibres with limited inflammatory infiltration. The inset shows vesicular nuclei with irregular outline. **(e)** Combined ALB/L-arginine-treated (G5) shows regular architecture of cardiomyocytes with very minimal inflammation. **(f)** High magnification of the myocardial cells of ALB/L-arginine-treated (G5) showing oval centrally placed myocardial nuclei. The myocardial fibres are seen separated by narrow inter-fibrillar spaces containing elongated and spindle-shaped nuclei of fibroblasts **(f)**, intercalated discs (spiral arrows) can also be observed. **f:** fibroblasts, **I:** inflammatory infiltration, **n:** nuclei. [**a,b,c,d,e:** magnification x400, scale bar 50 µm, and **f:** magnification x1000, scale bar 20 µm].

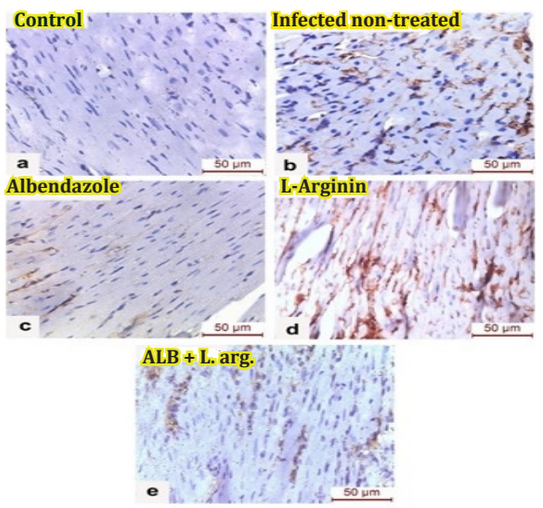

Fig. 5. Immunohistochemical expression of iNOS in the gastrocnemius muscle. **(a)** control (G1), **(b)** infected non-treated (G2), **(c)** ALB-treated (G3), **(d)** L-arginine-treated (G4), **(e)** combined ALB/L-arginine-treated (G5).

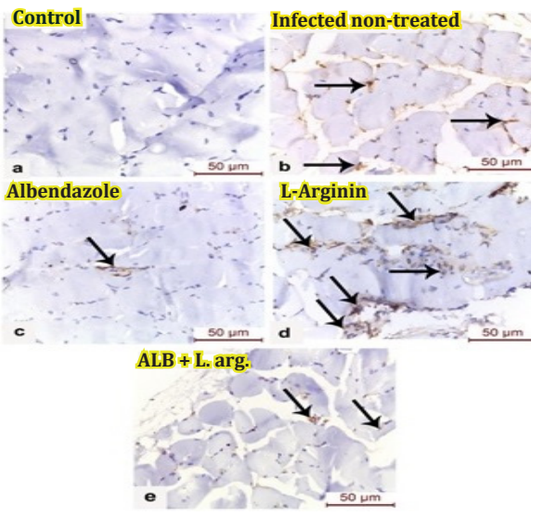

Fig. 6. Immunohistochemical expression of iNOS in the diaphragm. **(a)** Control (G1), **(b)** Infected non-treated (G2), **(c)** ALB-treated (G3), **(d)** L-arginine-treated (G4), **(e)** Combined ALB/L-arginine-treated (G5) (arrows indicating positive immunoreactivity).

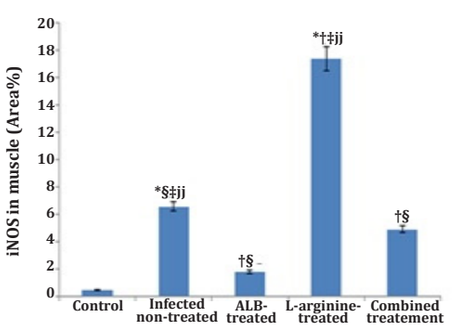

Fig. 7. Bar chart representing the percentage of iNOS expression in the gastrocnemius muscle in the different study groups. Statistical significance relative to ***:** control (G1), **†:** infected non-treated (G2), **‡:** ALB-treated (G3), **§:** L-arginine-treated (G4), **jj:** combined ALB and L-arginine-treated (G5).

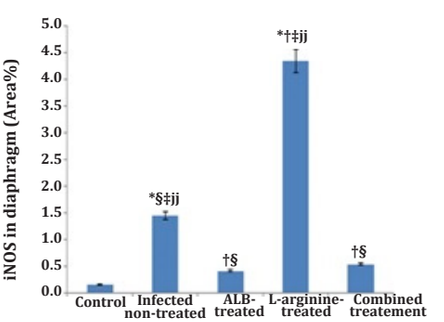

Fig. 8. Bar chart representing percentage of iNOS expression in the diaphragm in the different study groups. Statistical significance relative to ***:** control (G1), **†:** infected non-treated (G2), **‡:** ALB-treated (G3), **§:** L-arginine-treated (G4), **jj:** combined ALB and L-arginine-treated (G5).

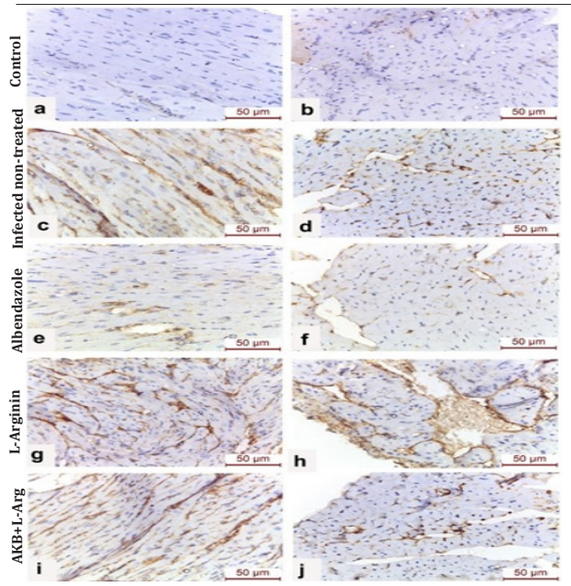

Fig. 9. Immunohistochemical expression of iNOS in the myocardium. **(a, b)** negative control (G1), **(c, d)** infected non-treated (G2). **(e, f)** ALB -treated (G3), **(g, h)** L-arginine-treated (G4). **(i, j)** combined ALB /L-arginine-treated (G5).

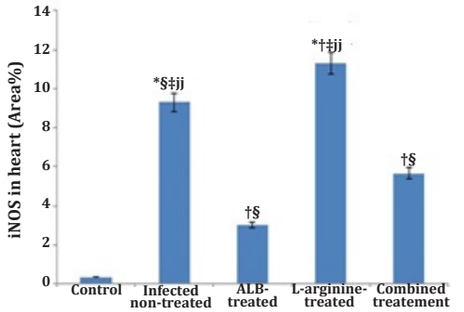

Fig. 10. Bar chart representing percentage of iNOS expression in the heart in the different study groups. Statistical significance relative to ***:** control (G1), **†:** infected non-treated (G2), **‡:** ALB-treated (G3), **§:** L-arginine-treated (G4), **jj:** combined ALB and L-arginine-treated (G5).

NO level in blood samples withdrawn during the muscle phase of infection was lowest in ALB-treated mice (G3) and highest in L-arginine-treated ones (G4). In the combined ALB/L-arginine therapy (G5), NO level was significantly reduced in comparison to the control (G1). Pairwise comparisons between the various study groups showed statistically significant difference except when comparing ALB monotherapy and combined ALB/L-arginine therapy, where no statistical significance was found between their serum NO levels (Table 4).

Effect of ALB and/or L-arginine on the gene expression of TNF-α and IFN-γ: TNF-α and IFN-γ were significantly higher in ALB-treated (G3) mice as compared to control infected non-treated (G2) mice. Combined ALB-arginine therapy (G5) resulted in a more significant increase in TNF-α and IFN-γ expression levels, while the highest levels were detected in L-arginine-treated (G4) mice (Table 5).

Table 4. Serum NO values detected in the different study groups.

Parameter		Non-infected control (G1)	Infected non-treated (G2)	ALB-treated (G3)	L-arginin-treated (G4)	Combined treatment (G5)	*P* value
Serum NO (*u*M)	**Mean**	1.75	118.75[T]	5.0 [I, L]	169.5 [I, A, C]	8.5 [I, L]	<0.001*
	SD	0.86	4.86	3.37	11.73	4.65	

***** Statistical significance. **A:** Statistical significance relative to ALB-treated (G3); **C:** Statistical significance relative to combined group (G5); **I:** Statistical significance relative to infected non-treated (G2); **L:** Statistical significance relative to L-arginine (G4); **T:** Statistical significance relative to all the treated groups.

Table 5. Relative expression levels of TNF-α and IFN-γ detected in the different study groups.

Parameter		Non-infected control (G1)	Infected non-treated (G2)	ALB-treated (G3)	L-arginin-treated (G4)	Combined treatment (G5)	*P* value
TNF-α	**Mean**	0.80 [T]	2.00 [T]	4.50 [I, L, C]	12.00 [I, L, C]	7.00 [I, A, L]	<0.001*
	SD	0.00	0.00	0.58	1.41	1.00	
IFN-γ	**Mean**	0.50 [T]	1.50 [T]	4.50 [I, L, C]	12.75 [I, A, C]	12.75 [I, A, L]	<0.001*
	SD	0.08	0.58	0.58	1.71	1.71	

***:** Statistical significance; **A:** Statistical significance relative to ALB group; **C:** Statistical significance relative to combined group (G5); **I:** Statistical significance relative to infected non-treated (G2); **L:** Statistical significance relative to L-arginine-treated (G4); **T:** Statistical significance relative to all the treated groups.

DISCUSSION

The immune response to *T. spiralis* is diverse and multi-orchestrated. This distinct nematode challenges the mucosal immune system, the systemic immune response, and the local tissue defense mechanism during the muscle phase. The anti-*Trichinella* immune response is thus a complex interplay between innate and acquired humoral and cellular immune responses[1,3]. In the current study, we investigated the effect of the antiparasitic drug ALB on the host immune response and the impact of the NO precursor L-arginine on parasitic burden, skeletal and myocardial muscle pathology, serum NO levels and gene expression levels of TNF-α and IFN-γ.

In our study, ALB was administered at a dose of 50 mg/kg on day 21 PI for five days and mice were sacrificed at day 30 PI. This resulted in induced larval degeneration and significant decrease in the larval count in infected muscles of mice by 95.5%, as compared to the non-treated control group. Several studies with different dosage regimen reported various reduction rates after ALB administration. Attia *et al*.[7] administered ALB to *Trichinella*-infected mice on day 31 PI for seven days and performed a larval count on day 49 PI. They reported a 90.9% reduction in parasitic burden. Nada *et al*.[27], on the other hand, reported 80.0% reduction in muscular larval count on day 35 PI after the administration of 50 mg/kg ALB on day 3 PI for 3 d. In our study, the combination of ALB with the amino acid L-arginine, led to a significant compromise in ALB efficacy (from 95.5% in ALB monotherapy to 69.6% in combined ALB/L-arginine therapy). Moreover, L-arginine monotherapy resulted in an increase in larval count by 51.8%. We also investigated the histopathological effect of ALB and L-arginine on infected mice. ALB was found to decrease the local inflammatory response, an effect slightly weakened by the addition of L-arginine. On the other hand, L-arginine resulted in an aggravation of the local inflammatory reaction around the larvae by augmenting capsular and interstitial infiltration. This was also associated with a significantly higher local iNOS expression and serum NO level in comparison to control mice, and in contrast to ALB-treated mice that showed significantly lower iNOS and NO levels. Lazer *et al*.[28] explained the anti-inflammatory action of benzimidazoles by their effect on neutrophil function, since this drug group inhibits the release of lysosomal enzymes from neutrophils. In opposition, the aggravating effect of L-arginine on *T. spiralis* infection and inflammatory reaction may be related to the action of NO on the immune response as was previously reported by Hadaś *et al*.[29] who explained their finding by the potential of high NO levels to dampen the immune response through the effect of nitrative stress. Similarly, Wandurska-Nowak *et al*.[30], in their study on NO-releasing drugs in murine trichinosis, suggested that the increased parasite burden may be related to the immunosuppressive effect of high doses of NO.

Larval degeneration was found in all drug-treated muscle samples, being most pronounced in samples from mice receiving ALB only. While the degenerative effect of ALB could be attributed to its direct effect on larval β-tubulin monomer, larval degeneration observed in L-arginine-treated mice could be explained by the anti-parasitic effect of NO[13]. Targeting parasite enzymes, especially cysteine proteases, by NO, leads to loss of enzyme activity and subsequently decreased viability of the invading pathogen[31].

Essential processes in the regeneration of an injured muscle are the proliferation of satellite cells and vascularization. The NO has a crucial role in this process as it acts as an intracellular signaling molecule and vasodilator, which can stimulate the secretion of several growth factors such as VEGF and basic fibroblast growth factor (bFGF). In our work, the effect of L-arginine on muscle degeneration was found to be particularly interesting, as degeneration was not encountered in the examined muscle samples of L-arginine-treated mice, although degeneration was observed in ALB-treated mice and to a lesser extent in the combined ALB/L-arginine regimen. A histopathological effect was observed in heart sections of L-arginine treated mice, where myocardial fibers displayed minimal inflammation and intact fibers. In opposition, the infected non-treated group showed areas of cardiomyocyte degeneration which were replaced by dense inflammatory cellular infiltration. In a study by Paolocci *et al*.[32], histopathological sections of the hearts of rats infected with *T. spiralis* displayed scattered foci of eosinophilic and mononuclear inflammatory infiltrates, in addition to necrosis and fiber disarrangement. In another study, the effect of L-arginine on experimentally induced autoimmune myocarditis was studied. L-arginine was found to have an anti-inflammatory and cardioprotective effect by maintaining the extracellular matrix structure and decreasing the cytotoxicity of inflammatory cells[33].

The effect of L-arginine on skeletal muscle regeneration was studied by Hnia *et al*.[34] in mdx mice, which are a mice model homologous to Duchenne muscular dystrophy and are used to study related aspects of pathogenesis. Of particular relevance to our study was the effect of L-arginine, which was found to promote muscle membrane integrity in dystrophic muscles. Filippin *et al*.[35] demonstrated the effect of NO on muscle regeneration by examining the effect of L-NAME, a NO inhibitor, on an experimental model of muscular injury. L-NAME was found to decrease inflammatory cellular infiltration and induce focal areas of fibrosis. This may reflect the influence of NO on the early process of regeneration through its effect on inflammatory cells and their growth factors and cytokines thus activating the quiescent satellite cells and the muscle repair process. Nitric oxide thus acts as a regulator of the balance between fibrosis and muscle regeneration. Boczoń *et al*.[36] studied the effect of NO during the muscular phase of infection by tracing the expression of iNOS. Enzyme expression was detected at both the mRNA and protein levels starting on day 21 PI. Inducible NOS-positive cells included mainly tissue macrophages and T-lymphocytes. The demonstration of iNOS activity in muscle tissue during the muscular phase of trichinosis reflects the important role of NO during the course of muscular infection. In our study, ALB was associated with local iNOS and serum NO levels that were lower than those found in infected non-treated mice. In a study by Nassef *et al*.[37], Chitosan nanoparticles loaded with ALB resulted in decreased iNOS expression in mice infected with trichinosis. A stimulatory effect of ALB on enzymes involved in

oxidative and nitrative stress has been described in another study[38]. Castro *et al*.[39] proposed that ALB, through the induction of oxidative stress, promotes DNA fragmentation and triggers apoptosis and cell death. Apoptotic cells have been found to induce anti-inflammatory mediators and suppress NO synthesis in murine macrophages[40].

The importance of arginine in innate immunity is not merely attributed to its role as a NO precursor. Arginine metabolism also determines the polarization of the immune response towards the pro-inflammatory M1 macrophages responsible for the dominance of a Th-1 environment, as opposed to the anti-inflammatory M2 macrophages that favor an anti-parasitic Th-2 response. While M1 macrophages produce NO, M2 macrophage on the other hand decrease NO production by the suppression of iNOS expression and alternative production of arginase, which breaks down arginine to ornithine and urea. This polarization effect is orchestrated by pro- and anti-inflammatory cytokines. Among the pro-inflammatory cytokines favoring the M1 pro-inflammatory pathway are TNF-α and IFN-γ[41]. Salim *et al*.[42] studied the effect of TNF-α and IFN-γ on iNOS gene expression by creating a comprehensive kinetic macrophage environment, where signal transduction, gene expression and metabolic outcomes were assessed. They concluded that both cytokines act in a synergistic manner, since TNF-α achieves a rapid iNOS induction response, whereas IFN-γ results in the priming of that response to a maximum effective expression level.

Increased gene expression of TNF-α and IFN-γ detected in our study reflects their active role during the disease process and the influence of the investigated drugs on their expression. Samples from mice treated with ALB and/or L-arginine were found to show significantly higher expression levels of TNF-α and IFN-γ as compared to control infected non-treated samples, with the increase in L-arginine-treated samples being more pronounced. Enhanced gene expression in L-arginine-treated samples might be part of the overall synergy of a pro-inflammatory response; or may point to a possible direct effect on the gene expression machinery during infection[43]. Similarly, the expression levels of TNF-α and IFN-γ were higher in ALB-treated samples as compared to control samples, which sheds light on the possible immune-mediated mechanisms of ALB other than the well-known direct effect on parasite β-tubulin. In a study by Wang *et al*.[44], the mechanism of cytotoxicity of ALB on human leukaemia cells U 937 was investigated. Albendazole-induced apoptosis was found to be mediated in part by mitochondrial oxidative stress in addition to the upregulation of TNF-α.

In conclusion, studying the effect of ALB on the peculiar niche environment of muscular trichinosis in view of the presence of the NO donor L-arginine provides valuable insight into the complex relation between iNOS expression and NO production, the pro-inflammatory cytokine gene expression, and the local inflammatory response. Investigation of alternative ALB modes of action involving the host immune mechanisms may pave the way for better medication therapy tailoring based on the immunological condition of the host. In addition, the role of adjuvant immunomodulatory therapy should be highlighted. The effect of amino acids such as L-arginine that could affect the immune system in general and the NO production in particular, on the outcome of parasitic infections should be thoroughly investigated. The regenerative effect of L-arginine on muscle fibers and its possible cardioprotective effect advocates this amino acid as a beneficial supplement in chronic *Trichinella*-induced myositis and myocarditis. The importance of L-arginine is not just because of its critical role as a NO precursor and a driver of immune response polarization, but also because it is a semi-essential amino acid found in a variety of foods and supplements.

Author contribution: Abdeltawab MSA, Wanas H, Abdel-Shafi IR, and Hamed AMR developed the study concept and design, prepared the material, implemented the experiment, and provided animal care. Saad El-Din SS prepared the material and implemented the molecular assessment of TNF-α and IFN-γ gene expression and assessment of serum NO level. Aboulhoda BE prepared the material and implemented the immunohistochemical assessment of iNOS expression and histopathological examination. Amer SII prepared the material and implemented the histopathological examination. Abdeltawab MSA, Abdel-Shafi IR, and Hamed AMR A, analyzed data. All authors shared in the writing of the original draft of the manuscript and the final reviewing and editing. All authors critically revised and approved the final manuscript.

Conflicts of interest: The authors declare that they have no conflict of interest.

Financial support: No source of funding.

REFERENCES

1. Sofronic-Milosavljevic L, Ilic N, Pinelli E Gruden-Movsesijan A. Secretory products of *Trichinella spiralis* muscle larvae and immunomodulation: implication for autoimmune diseases, allergies, and malignancies J Immunol Res 2015;523875.
2. Gottstein B, Pozio E, Nöckler K. Epidemiology, diagnosis, treatment, and control of trichinellosis. Clin Microbiol Rev 2009; 22(1):127-145.
3. Wu Z, Sofronic-Milosavljevic L, Nagano I, Takahashi Y. *Trichinella spiralis*: Nurse cell formation with emphasis on analogy to muscle cell repair. Parasite Vectors 2008; 1:27.
4. Albakri A. Parasitic (Helminthic) cardiomyopathy a review and pooled analysis of pathophysiology,

diagnosis, and clinical management. Med Clin Arch 2019; (3):1000153.
5. Fabre MV, Beiting DP, Bliss SK, Appleton JA. Immunity to *Trichinella spiralis* muscle infection. Vet Parasitol 2009; 159(3-4):245-248.
6. Beiting DP, Gagliardo LF, Hesse M, Bliss SK, Meskill D, Appleton JA. Coordinated control of immunity to muscle stage *Trichinella spiralis* by IL-10, regulatory T cells, and TGF-β. J Immunol 2007; 178(2):1039-1047.
7. Attia RA, Mahmoud AE, Farrag HM, Makboul R, Mohamed ME, Ibraheim Z. Effect of myrrh and thyme on *Trichinella spiralis* enteral and parenteral phases with inducible nitric oxide expression in mice. Mem Inst Oswaldo Cruz 2015;110 (8): 1035-1041.
8. Castro IC, Oliveira BB, Slowikowski JJ, Coutinho BP, Siqueira FJW *et al*. Arginine decreases *Cryptosporidium parvum* infection in undernourished suckling mice involving nitric oxide synthase and arginase. Nutrition 2012; 28(6):678-685.
9. Mirmiran P, Bahadoran Z, Ghasemi A Azizi F. The association of dietary L-arginine intake and serum nitric oxide metabolites in adults: A population-based study. Nutrients 2016; 8(5):311.
10. James SL. Role of nitric oxide in parasitic infections. Microbiol Mol Biol Rev 1995; 59(4):533-547.
11. Das P, Lahiri A, Lahiri A, Chakravortty D. Modulation of the arginase pathway in the context of microbial pathogenesis: A metabolic enzyme moonlighting as an immune modulator. PLoS Pathog 2010; 6(6): e1000899.
12. Stadelmann B, Hanevik K, Andersson MK, Bruserud O, Svärd SG. The role of arginine and arginine-metabolizing enzymes during *Giardia*–host cell interactions *in vitro*. BMC Microbiol 2013;13:256.
13. Lacey E. The mode of action of Benzimidazoles. J Parasitol Today 1990; 6 (4):112-115.
14. Diao Z, Chen X, Yin C, Wang J, Qi H, Ji A. *Angiostrongylus cantonensis*: effect of combination therapy with albendazole and dexamethasone on Th cytokine gene expression in PBMC from patients with eosinophilic meningitis. Exp Parasitol 2009;123(1):1-5.
15. McCracken RO. Efficacy of mebendazole and albendazole against *Trichinella spiralis* in mice. J Parasitol 1978; 64(2):214-219.
16. Chung, MS, Joo KH, Quan FS, Kwon HS, Cho KH. Efficacy of flubendazole and albendazole against *Trichinella spiralis* in mice. Parasite 2001; 2(2):S195-S198.
17. Albayati MA, Ahmad MA, Khamas W. The potential effect of L-arginine on mice placenta. Pharmacoepidemiol Drug Saf 2014; 3(2):1000150.
18. Fadl HO, Amin NM, Wanas H, El-Din SS, Ibrahim HA, Aboulhoda BE, *et al*. The impact of L-arginine supplementation on the enteral phase of experimental *Trichinella spiralis* infection in treated and untreated mice. J Parasit Dis 2020;44(4):737–747.
19. Cormack DH. Essential histology. 2nd ed. Lippincott Williams & Wilkins, USA, 2001. 456 p.
20. Ashour DS, Rayia DMA, Saad A E, El-Bakary RH. Nitazoxanide anthelmintic activity against the enteral and parenteral phases of trichinellosis in experimentally infected rats. Exp Parasitol 2016; 170: 28-35.
21. Sek AC, Moore IN, Smelkinson MG, Pak K, Minai M, Smith R, *et al*. Eosinophils do not drive acute muscle pathology in the mdx mouse model of Duchenne Muscular Dystrophy. J Immunol Res 2019; 203 (2):476-484.
22. Bancroft JD , Gamble M. Theory and practice of histological techniques. 5th ed. Churchill Livingstone Elsevier, USA, 2002; 796 p.
23. El Asar HM, Mohammed EA, Aboulhoda EA, Emam HY, Imam AA. Selenium protection against mercury neurotoxicity: Modulation of apoptosis and autophagy in the anterior pituitary. Life Sci 2019; 231:116578.
24. Onaolapo, Olakunle J. l-Methionine and silymarin: A comparison of prophylactic protective capabilities in acetaminophen-induced injuries of the liver, kidney and cerebral cortex, Biomed Pharmacother 2017; 85:323-333.
25. Schmittgen TD, Livak KJ. Analyzing real-time PCR data by the comparative CT method. Nat Protoc 2008; 3(6):1101-8.
26. Etti IC, Abdullah R, Kadir A, Hashim NM, Yeap SK, Imam MU, *et al*. The molecular mechanism of the anticancer effect of Artonin E in MDA-MB 231 triple negative breast cancer cells. PLoS ONE 12(8):e0182357.
27. Nada SM, Mohammad SM, Ibrahim N. Therapeutic effect of *Nigella sativa* and ivermectin versus albendazole on experimental trichinellosis in mice. JESP 2018; 48(1):85-92.
28. Lazer ES, Matteo MR, Possanza GJ. Benzimidazole derivatives with atypical anti-inflammatory activity. J Med Chem 1987; 3 (4):726-729.
29. Hadaś E, Derda M,Wandurska-Nowak E. Effect of exogenous nitric oxide in experimental trichinellosis. J Parasitol Res 2002; 88(1): 86-88.
30. Wandurska-Nowak E, Hadaś E, Derda M Wojt W. Effect of nitric oxide releasing drugs on the intensity of infection during experimental trichinellosis in mice. Parasitol Res 2003; 90(2):164-165.
31. Ascenzi P, Bocedi A, Gradoni L. The anti-parasitic effects of nitric oxide. IUBMB Life 2003; 55(10-11): 573-578.
32. Paolocci N, Sironi M, Bettini M, Bartoli G, Michalak S, Bandi C, *et al*. Immunopathological mechanisms underlying the time-course of *Trichinella spiralis* cardiomyopathy in rats. Virchows Archiv 1998; 432:261-266.
33. Okabe TA, Hattori M, Yuan Z, Kishimoto C. L-arginine ameliorates experimental autoimmune myocarditis by maintaining extracellular matrix and reducing cytotoxic activity of lymphocytes. Int J Exp 2008; 89:382-388.
34. Hnia K, Gayraud J, Hugon G, Ramonatxo M, De La Porte S, Matecki S, Mornet D. L-arginine decreases inflammation and modulates the nuclear factor-κB/ matrix metalloproteinase cascade in mdx muscle fibers. Am J Clin Pathol 2008; 172(6):1509-1519.
35. Filippin LI, Cuevas MJ, Lima E, Marroni NP, Gonzalez-Gallego JR, Xavier M. Nitric oxide regulates the repair

of injured skeletal muscle. Nitric Oxide 2011; 24(1):43-49.
36. Boczoń K, Wandurska-Nowak E, Wierzbicki A, Frydrychowicz M, Mozer-Lisewska I, Zeromski J. mRNA expression and immunohistochemical localization of inducible nitric oxide synthase (NOS-2) in the muscular niche of *Trichinella spiralis*. Folia Histochem Cytochem 2004; 42(4):209-213.
37. Nassef NE, Moharm IM, Atia AF, Barakat RM, Abou Hussein NM, Mohamed AS. Therapeutic efficacy of chitosan nanoparticles and albendazole in intestinal murine trichinellosis. JESP 2018;48(3):493-502.
38. Żeromski J, Boczoń K, Wandurska-Nowak E, Mozer-Lisewska I. Effect of aminoguanidine and albendazole on inducible nitric oxide synthase (iNOS) activity in *T. spiralis*-infected mice muscles. Folia Histochem Cytobiol 2005; 43(3):157-159.
39. Castro LM, Kviecinski R, Ourique F, Parisotto EB, Grinevicius VS *et al*. Albendazole as a promising molecule for tumor control. Redox Biol 2016; 10:90-99.
40. Freire-de-Lima CG, Xiao QY, Gardai SJ, Bratton BL, Schiemann WP, Henson PM. Apoptotic cells, through transforming growth factor-β, coordinately induce anti-inflammatory and suppress pro-inflammatory eicosanoid and NO synthesis in murine macrophages. J Biol Chem 2006; 281(50):38376-38384.
41. Gogoi M, Datey A, Wilson KT, Chakravortty D. Dual role of arginine metabolism in establishing pathogenesis. Curr Opin Microbiol 2016; 29:43-48.
42. Salim T, Sershen CL, May EE Investigating the role of TNF-α and IFN-γ activation on the dynamics of iNOS gene expression in LPS stimulated macrophages. PloS ONE 2016;11(6):e0153289.
43. Shang HF, Hsu CS, Yeh CL, Pai MH, Yeh SL. Effects of arginine supplementation on splenocyte cytokine mRNA expression in rats with gut-derived sepsis. World J Gastroenterol 2005; 11(45):7091-7096.
44. Wang LJ, Lee YC, Huang CH, Shi YJ, Chen YJ *et al*. Non-mitotic effect of albendazole triggers apoptosis of human leukemia cells via SIRT3/ROS/p38 MAPK/TTP axis-mediated TNF-α upregulation. Biochem Pharmacol 2019;162:154-168.